Quantifying the impact of the North American monsoon and deep midlatitude convection on the subtropical lowermost stratosphere using in situ measurements

E. M. Weinstock,[1] J. V. Pittman,[1,2] D. S. Sayres,[1] J. B. Smith,[1] J. G. Anderson,[1] S. C. Wofsy,[3] I. Xueref,[3,4] C. Gerbig,[3,5] B. C. Daube,[3] L. Pfister,[6] E. C. Richard,[7] B. A. Ridley,[8] A. J. Weinheimer,[8] H.-J. Jost,[6,9] J. P. Lopez,[6] M. Loewenstein,[6] and T. L. Thompson[10]

Received 16 February 2007; revised 22 May 2007; accepted 2 July 2007; published 26 September 2007.

[1] The chemical composition of the lowermost stratosphere exhibits both spatial and temporal variability depending upon the relative strength of (1) isentropic transport from the tropical tropopause layer (TTL), (2) diabatic descent from the midlatitude and northern midlatitude stratosphere followed by equatorward isentropic transport, and (3) diabatic ascent from the troposphere through convection. In situ measurements made in the lowermost stratosphere over Florida illustrate the additional impact of equatorward flow around the monsoon anticyclone. This flow carries, along with older stratospheric air, the distinct signature of deep midlatitude convection. We use simultaneous in situ measurements of water vapor (H_2O), ozone (O_3), total odd nitrogen (NOy), carbon dioxide (CO_2), and carbon monoxide (CO) in the framework of a simple box model to quantify the composition of the air sampled in the lowermost stratosphere during the mission on the basis of tracer mixing ratios ascribed to the source regions for these transport pathways. The results show that in the summer, convection has a significant impact on the composition of air in the lowermost stratosphere, being the dominant source of water vapor up to the 380 K isentrope. The implications of these results extend from the potential for heterogeneous ozone loss resulting from the increased frequency and lifetime of cirrus near the local tropopause, to air with increased water vapor that as part of the equatorward flow associated with the North American monsoon can become part of the general circulation.

Citation: Weinstock, E. M., et al. (2007), Quantifying the impact of the North American monsoon and deep midlatitude convection on the subtropical lowermost stratosphere using in situ measurements, *J. Geophys. Res.*, *112*, D18310, doi:10.1029/2007JD008554.

1. Introduction

[2] Elucidating the critical link between UV dosage and climate change requires an understanding of the coupling of dynamics, chemistry, and radiation especially within the tropical tropopause layer (TTL), the midlatitude upper troposphere, and the lowermost and lower stratosphere. Measurements of the distribution of long-lived tracers of transport, and short-lived tracers of chemical activity within this region, provide the basis for validating models and testing this understanding. The objective of this paper is to develop and test a framework in which high-resolution in situ chemical tracer measurements can be used to enhance our understanding of the transport pathways and dynamical mechanisms that control the distribution of tracers within this domain as a function of latitude, longitude, and season.

[3] The lowermost stratosphere, the region in the extratropics bounded from above by the isentrope corresponding to the tropical tropopause, typically 380–390 K, and from below by the local tropopause, is a critical part of this domain. For example, vertical profiles of ozone in northern midlatitudes [*Logan et al.*, 1999] showed a decrease of about 1%/year in late winter and early spring during the 1980s and 1990s, with the maximum percentage ozone loss

[1]Department of Chemistry and Biological Chemistry, Harvard University, Cambridge, Massachusetts, USA.
[2]Now at NASA Marshall Space Flight Center, Huntsville, Alabama, USA.
[3]Department of Earth and Planetary Sciences, Harvard University, Cambridge, Massachusetts, USA.
[4]Now at Laboratoire des Sciences du Climat et de l'Environment, Commissariat l'Energie Atomique, Gif-Sur-Yvette, France.
[5]Now at Max-Planck Institute for Biogeochemistry, Jena, Germany.
[6]NASA Ames Research Center, Moffett Field, California, USA.
[7]Laboratory for Atmospheric and Space Physics, University of Colorado, Boulder, Colorado, USA.
[8]Atmospheric Chemistry Division, National Center for Atmospheric Research, Boulder, Colorado, USA.
[9]Now at NovaWave Technologies, Redwood City, California, USA.
[10]Earth System Research Laboratory, NOAA, Boulder, Colorado, USA.

0148-0227/07/2007JD008554

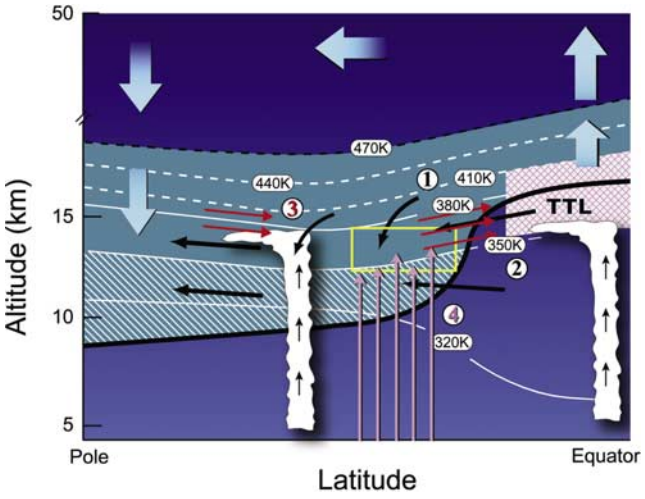

Figure 1. A plot of isentropic surfaces as a function of latitude and altitude. Transport into a section of the lowermost stratosphere within the rectangle illustrated here, is represented by the heavy black arrows, typically resulting in a mixture of stratospheric air (path 1) and tropospheric air (path 2). The horizontal red arrows, pointing equatorward, represent the potential for isentropic transport of northern latitude air to the midlatitudes, subtropics, and even into the tropics (path 3). The purple vertical arrows represent local convection, which typically transports air into the upper troposphere, and on occasion into the lowermost stratosphere (path 4). Nonlocal convection is represented by the black vertical arrows within the midlatitude and tropical convective clouds (path 4). The large light blue arrows represent the general circulation and are included for completeness.

occurring in the lowermost stratosphere. *Bojkov and Fioletov* [1997] reduce the uncertainty of calculated trends in the lowermost stratosphere by analyzing ozone changes as a function of altitude from the locally determined tropopause. Their analysis shows that the negative stratospheric trends become significant 1–2 km above the tropopause.

[4] To explore the relative importance of dynamical and chemical components to an ozone trend, any framework we establish must be suitable for quantifying the importance of the different source regions that supply air to the lowermost stratosphere, while incorporating the range of their respective ozone mixing ratios, as well as water vapor and short-lived species that catalytically remove ozone, and enabling assessment of their sensitivity to climate forcing. Transport of air throughout this region is generally described in the context of a plot of isentropes as a function of latitude and altitude [*Holton et al.*, 1995]. We illustrate a version of this type of diagram in Figure 1 where we focus on a section of the lowermost stratosphere within the rectangle to represent the air sampled during Cirrus Regional Study of Tropical Anvils and Cirrus Layers–Florida Area Cirrus Experiment (CRYSTAL-FACE). Descriptions of the transport pathways into and out of the lowermost stratosphere that are represented by the different arrows in Figure 1 are listed in the figure caption.

[5] The general thrust of aircraft-borne measurements [*Hintsa et al.*, 1994, 1998; *Boering et al.*, 1995, 1996; *Dessler et al.*, 1995] and balloon-borne measurements [*Ray et al.*, 1999] is that there is a seasonal dependence to the relative amounts of air moving via two paths into the lowermost stratosphere: poleward adiabatic transport from the tropical tropopause layer (path 2 in Figure 1); and diabatic descent from the tropical and subtropical stratosphere (path 1 in Figure 1). Equatorward isentropic transport (path 3 in Figure 1), influenced by monsoon circulation in both the eastern and western hemispheres [*Dunkerton*, 1995; *Bannister et al.*, 2004], was observed during CRYSTAL-FACE [*Richard et al.*, 2003; *Ray et al.*, 2004]. *Gettelman et al.* [2004] used a three-dimensional chemical transport model driven by observed winds along with satellite-based and CRYSTAL-FACE ozone and water vapor data to validate the parameterizations of the dynamical processes that impact tracer mixing ratios in the context of monsoon circulations.

[6] While Figure 1 does not show convection extending above 380 K into the overworld, evidence of convection into the lower stratosphere has previously been reported by *Poulida et al.* [1996]. *Jost et al.* [2004] used analyses of CRYSTAL-FACE data to identify midlatitude convective events that transport organic pollutants and water into the lower stratosphere as well. More recently, *Hanisco et al.* [2007] reported in situ measurements of water vapor isotopes over the Midwestern United States during northern midlatitude summer indicating that direct convection is a significant hydration source for the lower stratosphere.

[7] *Pittman et al.* [2007], in a study that provides results complementary to and consistent with those presented in this manuscript, used statistical techniques to qualitatively identify the origin and subsequent transport pathways of air sampled in the subtropical lowermost stratosphere during CRYSTAL-FACE. Their results indicated that most of the variability in the data can be explained by the stratospheric age of the air, followed by the age of the convective influence, and last by the extent of the convective influence, which has been hypothesized to be related to the latitude of convective injection [*Dessler and Sherwood*, 2004]. In order to explain the observed distribution of the different air masses identified in the region, *Pittman et al.* [2007] emphasized the critical role of the upper level circulation associated with the North American monsoon.

[8] *Dessler and Sherwood* [2004] use a single level semi-Lagrangian isentropic model with parameterized convection to simulate water and ozone on the 380-K surface in the Northern Hemisphere for the month of July from 1992 through 1999. Their goal was to analyze the effect of convection on the extratropical lower stratosphere, and they suggest a potential impact on the stratospheric water vapor budget that is dependent on convective mass flux. Because, as shown by *Dessler and Sherwood* [2004, Figure 3], the ice saturation mixing ratio (smr) on the 380 K surface strongly decreases with decreasing latitude, convection to the 380 K surface provides greater hydration potential at northern latitudes. However, this also suggests that the contribution from a northern midlatitude convective event to water vapor in an air parcel sampled in the subtropics is limited by the smr set by the cloud top temperature.

[9] For this manuscript, we use stratospheric and upper tropospheric tracer measurements taken during CRYSTAL-FACE as a means of quantifying the fraction of air from the source regions delineated in Table 1. The CRYSTAL-FACE

Table 1. List of Transport Pathways Depicted in Figure 1 for Air Entering the Lowermost Stratosphere, Along With the Corresponding Source Regions and Source Gas Designations for Each Region[a]

Pathway Number	Transport Pathway	Source Regions	Source Gas Designation
1	poleward with diabatic descent	lower tropical and subtropical stratosphere	young stratospheric air
2	poleward isentropic	tropical tropopause layer	tropical tropospheric air
3	equatorward transport (with convective input)	midlatitude and/or northern midlatitude stratosphere (with tropospheric contribution)	old stratospheric air (with convected air)
4	local convection	subtropical troposphere	convected air

[a]Corresponding to pathway 1, we use one source gas designation, young stratospheric air, to represent air in the lower tropical and subtropical stratosphere. However, pathway 3, which quasi-isentropically traverses the midlatitudes from 30 to 60°N in the lower stratosphere, can accordingly be the source of air from different latitudes. Additionally, it can be modified by convective injection along the way. There are therefore two source gas designations for air in the source region for transport pathway 3. We discuss in the model description section of the paper how well we can constrain the composition of the different convective source possibilities.

campaign took place during the month of July 2002 in Key West, Florida (23°N, 84°W), during which the NASA WB-57 aircraft flew 12 science flights in addition to the ferry flight from Houston to Key West. While most of the flights focused on the study of cirrus in the upper troposphere, flight trajectories often included climbs into the lower stratosphere, up to 440 K. As we show in Figure 2, back trajectories indicate that much of the air sampled in the lowermost stratosphere during CRYSTAL-FACE came from northern midlatitudes as part of anticyclonic flow around the North American monsoon. However, the fraction of that air that originated in the TTL, a potential, if not likely, source of air traveling poleward (path 1) along the western side of the anticyclone, is undetermined. Accordingly, this flow pattern provides an opportunity for air in the northern midlatitude lower stratosphere to be mixed with TTL air before it heads equatorward. Additionally, Figure 1 includes a convective contribution to lowermost stratospheric air, not only from local convection over Florida, but also from convective injection in the midlatitudes along back trajectories. Midlatitude convection could not only supply tropospheric air to the lowermost stratosphere, but also potentially provide

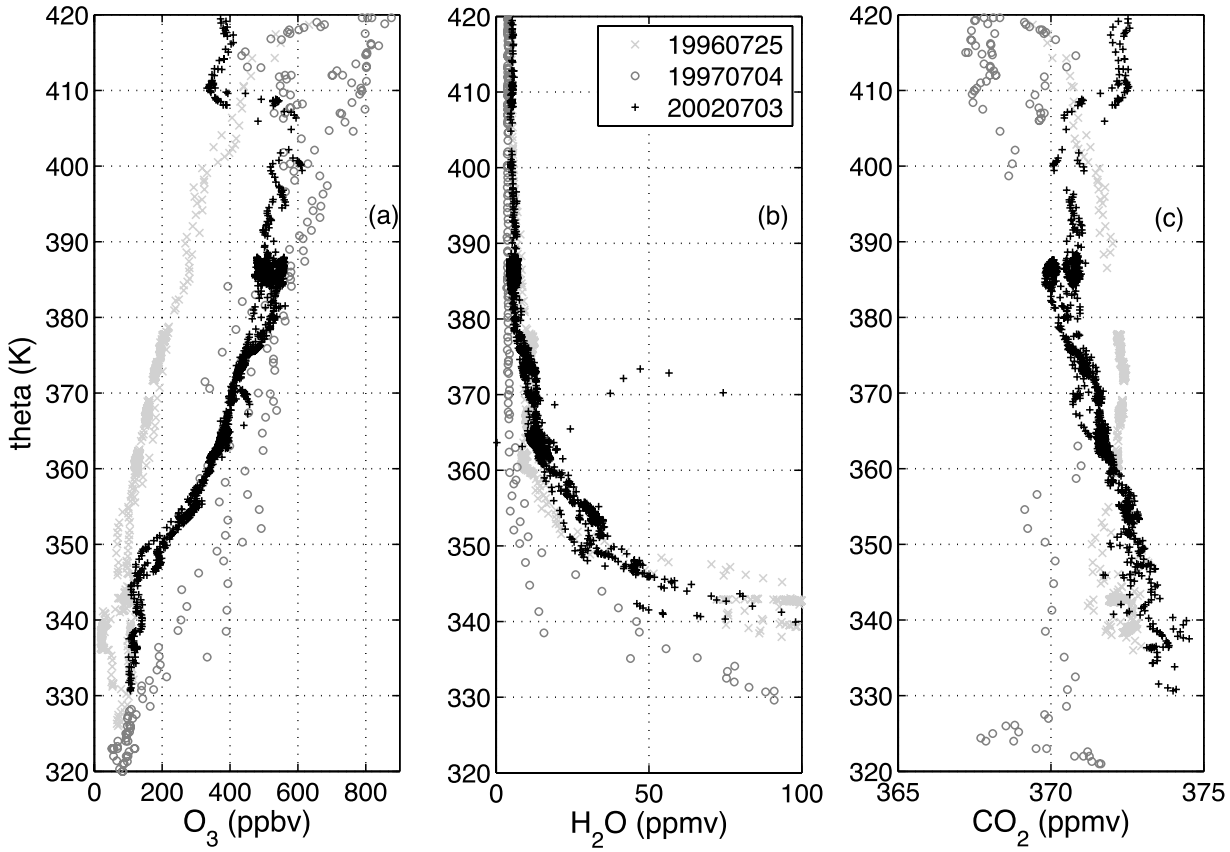

Figure 2. Tracer plots for the 20020703 flight during CRYSTAL-FACE compared with summer tracer profiles measured during the STRAT and POLARIS campaigns from NASA Ames Research Center, CA (37°N, 122°W). The STRAT and POLARIS CO_2 profiles are adjusted to account for the secular trend in stratospheric CO_2.

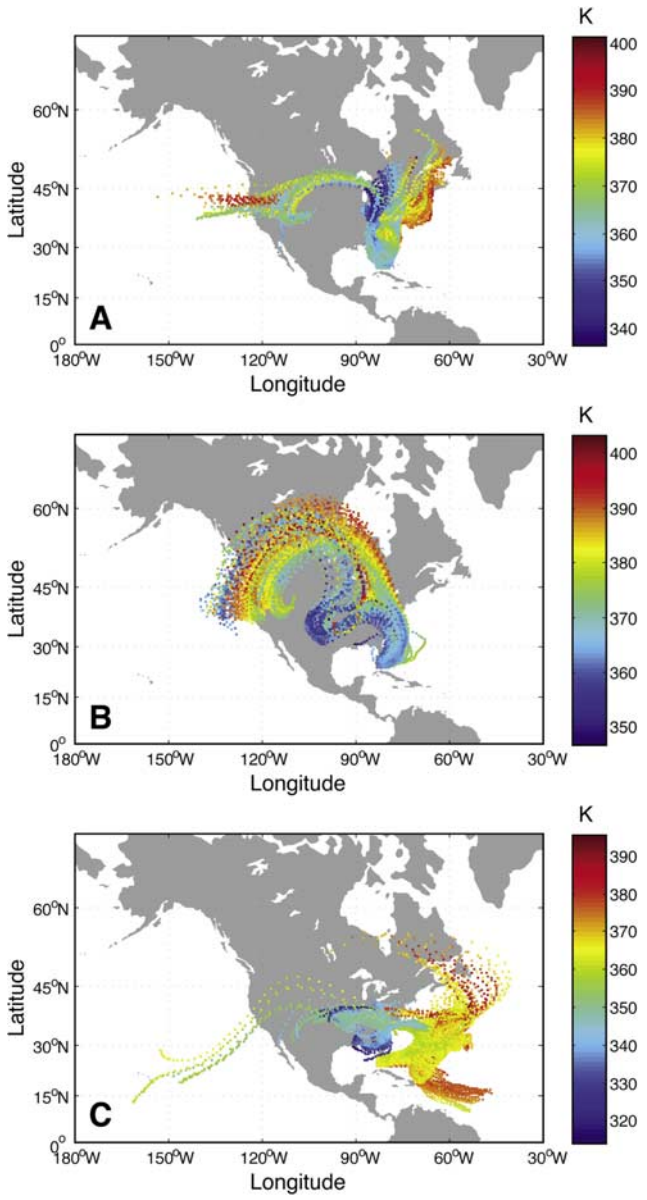

Figure 3. Plots of 7-day back trajectories calculated using the FABtraj model. (a) Initialized on 7 July 2002 (regime 1), (b) initialized on 19 July 2002 (regime 2), and (c) initialized on 28 July 2002 (regime 3). Color-coding is for potential temperatures (in K).

turbulent mixing [*Lane et al.*, 2003; *Wang*, 2003] that would enhance the entrainment of local stratospheric air and recently convected air into the monsoonal flow.

[10] The specific questions we quantitatively address in this manuscript are the following: (1) How did the equatorward flow around the monsoon impact the chemical composition of the lowermost stratosphere over Florida? (2) How much did convected air carried by the monsoonal flow impact the lowermost stratosphere during the same period? (3) How much did convected air carried by the monsoonal flow impact the lowermost stratosphere during the same period?

[11] The degree to which these results impact the lowermost stratosphere beyond the southeastern United States not only at midlatitudes but even into the TTL, and to what extent this will systematically change in a climate system forced by increasing CO_2, need to be fully explored.

2. CRYSTAL-FACE Tracer Data

[12] This section provides an example of how tracer data may be used to understand the coupling between the chemical composition and transport dynamics of the atmosphere. To provide context for the CRYSTAL-FACE tracer observations, we present in Figure 2 representative northern midlatitude summertime vertical profiles taken during the STRAT and POLARIS campaigns along with the comparable profile for the 20020703 flight that most clearly illustrates the impact of equatorward transport in the lowermost stratosphere. The STRAT data were taken on 25 July 1996 on the NASA ER-2 flight from the Ames Research Center (37°N, 122°W). Note that for the POLARIS data, the tropopause is at about 335 K, while for the STRAT and CRYSTAL-FACE data it is about 360 to 370 K. The plots of O_3 versus θ in Figure 2a illustrate the similarity between the air masses sampled during CRYSTAL-FACE and POLARIS from 360 to 400 K, with both plots showing much more O_3 than the plot of STRAT data. The plot of water vapor versus θ in Figure 2b shows that in the same region the profiles have varying degrees of water, with water in all profiles increasing below 360 K, and increasing from about 370 K in the 20020703 profile. The water vapor profiles plotted in Figure 2b show that the CRYSTAL-FACE air masses are much wetter than those sampled in POLARIS and STRAT. Together, these plots show that the air in the 20020703 flight might be a simple mixture of stratospheric and tropospheric air, with the data points falling on a mixing line between stratospheric air with 550 ppbv O_3 and about 5 ppmv water vapor and tropospheric air with 50 ppbv O_3 and 60 ppmv water vapor. We include a plot of CO_2 versus θ in Figure 2c. For this plot, CO_2 measured during STRAT and POLARIS was increased respectively by 9.5 and 8.0 ppmv to account for the secular trend in CO_2 of approximately 1.5 ppmv/year between 1996 and 2002 [*Conway et al.*, 2003]. Lower CO_2, similar to high O_3, shows evidence of the "older" stratospheric air sampled during the 20020703 flight, with the change in the character of the air starting at about 390 K.

[13] In order to examine the origin of the air over Florida on the basis of meteorological conditions, we show in Figure 3 seven-day backward trajectories using the FABtraj model [*Cooper et al.*, 2004]. Multiple trajectories are initialized within a volume that contains the location of the aircraft measurements obtained during three selected flights, each one corresponding to a regime identified by tracer analysis. The initial volume is located between 24 and 27°N, 80 and 83°W, within 145 and 105 hPa. The three days chosen, 7, 19, and 28 July, are days with trajectories that respectively represent the three trajectory regimes separately analyzed later in the manuscript. We reference the trajectories in Figure 3b, corresponding to 19 July, to explain how the various source regions contribute to the air mass sampled over Florida during CRYSTAL-FACE. While these seven-day back trajectories do not extend back into the tropics, we nevertheless assume that the sampled air parcels came out of the TTL with tropical character (path 2 in Figure 1). As an air parcel follows the monsoon circu-

lation poleward into northern midlatitudes it can be perturbed by strong local convection that promotes the mixing of recently convected air as well as older midlatitude air into the air parcel (path 3 in Figure 1). The strength, height, and proximity of the convection control the degree of mixing. The mixing of young stratosphere air into the lowermost stratosphere can be promoted by subtropical and extratropical convective mixing and can also occur all along its trajectory from the tropics to where it was sampled (path 1 in Figure 1). Because of the complexity of mixing processes, mixing from all of the source regions is allowed for each data point in every model run.

[14] To determine the composition of the air observed in the CRYSTAL-FACE profile, we assume that mixing takes place as subtropical air isentropically follows an anticyclonic flow poleward to northern latitudes and then equatorward. The original mix of upper tropospheric and lower stratospheric air originating in the TTL and exiting the subtropics mixes with young stratospheric air (similar to that observed during STRAT) and older stratospheric air (similar to that observed northward of the subtropical jet during POLARIS) as its trajectory traverses northern midlatitudes. While details of the processes causing the mixing are not available, it is plausible that midlatitude convective activity that occurs in northern midlatitudes in summer [see, e.g., *Jost et al.*, 2004; *Pittman et al.*, 2007], often penetrating the local tropopause, provides local turbulence [*Lane et al.*, 2003] that helps promote the mixing and adds convectively transported air as well. Because tracer isopleths slope downward with increasing latitude relative to isentropic surfaces, these convectively turbulent regions reach older stratospheric air. Additionally, as illustrated in Figure 1, while the CRYSTAL-FACE mission occurred by design over an area undergoing significant local convection, the convection rarely penetrated the local tropopause, and accordingly did not measurably affect the tracer composition of the lowermost stratosphere. Independent of the mixing mechanisms, or the extent of convective perturbation to the air masses sampled during CRYSTAL-FACE, we use simultaneous tracer measurements to determine the fraction of air corresponding to each of the source regions listed in Table 1 and linked to the air over Florida by the pathways outlined in Figure 1.

3. Mixing Model

3.1. Tracers Used in the Model

[15] Because we are interested in quantitatively differentiating between old and young stratospheric air, tropospheric air from the TTL, and that influenced by midlatitude or local convection, we choose five measured tracers, H_2O, O_3, CO_2, CO, and NOy, in the model with signatures that best correlate with each of these air mass descriptions. For example, stratospheric and tropospheric water vapor mixing ratios are easily distinguished, while water vapor mixing ratios are relatively invariant to the age of stratospheric air. On the other hand, O_3 is sensitive to stratospheric age and CO_2 is not only sensitive to stratospheric age because of its secular trend, but also provides additional selectivity with its seasonal cycle signature in young stratospheric air. CO is an excellent indicator of convection, and can also distinguish TTL air from stratospheric air, and with a stratospheric lifetime of less than six months, shows some sensitivity to the age of stratospheric air. Both NO and NOy resulting from lightning can be strong independent indicators of midlatitude or subtropical convective activity, as can (elevated) CO and (decreased) O_3. We do not use NO data to constrain the model output because of its short photochemical lifetime.

3.2. Source Region Profiles

[16] The ability of any tracer to distinguish the tracer origins can be most readily illustrated by plotting the source region profiles used in the model. We rely where possible on in situ tracer measurements to develop these profiles for the TTL and lower stratosphere. We show in Figure 4 sample source region profiles of the five tracers used in the mixing model. Profiles corresponding to different combinations of latitude and δK are used, as shown in the legend, where as previously described, δK represents the decrease in potential temperature of the tracer isopleths from the latitude to which the source profiles correspond to where they are used for isentropic mixing in the model. As stated previously, this downward adjustment of the profiles is consistent with the diabatic descent of stratospheric air in northern midlatitudes [*Strahan et al.*, 1998].

[17] For the TTL, all profiles with the exception of CO_2 are derived from averaged measurements in the TTL taken on the NASA ER-2 aircraft during the STRAT and POLARIS campaigns. For NOy, complications can potentially arise from convective influence. The TTL NOy profile in Figure 4 is an average of profiles that were not influenced by convection. It is possible that the air that originated in the TTL and was eventually sampled during CRYSTAL-FACE had fairly recently been over Central or South America, where the frequency of lightning flashes is about two orders of magnitude greater than over the tropical and subtropical ocean [*Christian et al.*, 2003]. In that case this NOy source profile could be underestimating the NOy contribution in the TTL air.

[18] The carbon dioxide TTL profile is derived from an average of the Mauna Loa and Samoa ground station data per *Boering et al.* [1994]. We assume immediate rapid ascent of the air mass from ground level to the 350 K isentrope, followed by an ascent rate of 0.5 K/day corresponding to 7.5 m/day through the TTL. The TTL water vapor profile has the largest uncertainty of all the tracers used, in part because of the possibility that relative humidities up to 1.6 [*Jensen and Pfister*, 2004; J. B. Smith et al., A climatology of aircraft-borne in situ observations of relative humidity in clear air and in cirrus, manuscript in preparation, 2007] relax constraints imposed by assumptions regarding dehydration to minimum saturation mixing ratios encountered on back trajectories, and in part from potential hydration from recent convection. We therefore check the model sensitivity to TTL water vapor by increasing the profiles by up to 50%. The significance of this uncertainty relates to the model's capability of distinguishing between isentropically transported TTL air and convected air. We also note that, as can be seen in Figure 4e, water vapor cannot help distinguish between young and old stratospheric air once there is any tropospheric input that significantly raises the water vapor mixing ratio well above stratospheric values.

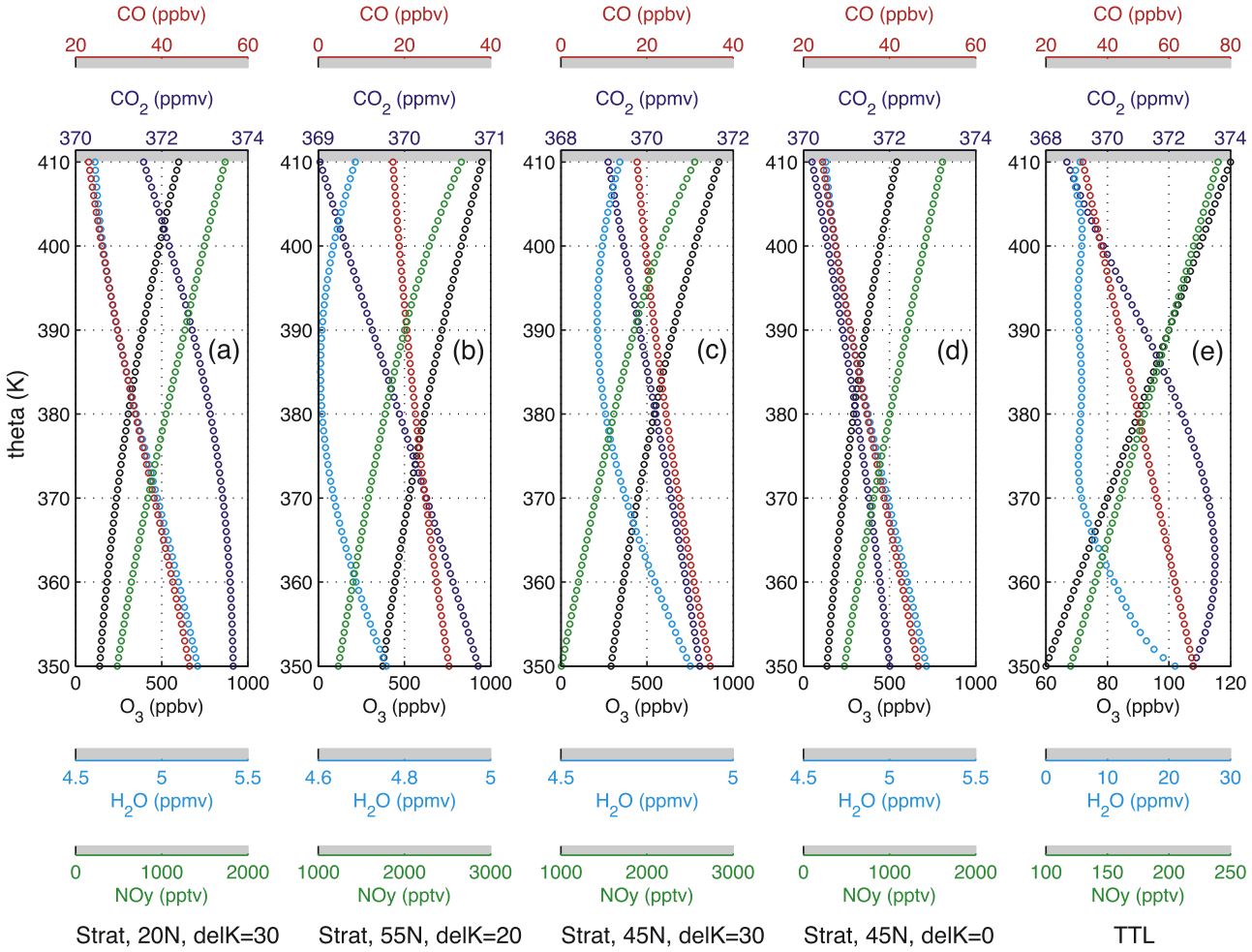

Figure 4. Sample source region profiles of (a) young stratospheric air (STRAT 20°N), (b–d) older stratospheric air, (STRAT 55°N and 45°N), and (e) tropical air (TTL), for use in the model. For Figures 4a–4d the plotted profiles are shifted downward by the designated δK from their measured θ values.

[19] The northern midlatitude lower stratosphere is the source region for air following path 3 in Figure 1. However, water vapor mixing ratios measured above 7 ppmv in this region provide evidence of tropospheric air mixed in with the stratospheric air preventing the use of those mixing ratios for pure stratospheric source region profiles. It is therefore necessary to develop stratospheric source region profiles using tracer mixing ratios measured above 390 K, which can descend into the lowermost stratosphere, following transport pathway 1 as illustrated in Figure 1. Air in this region, the lower midlatitude stratosphere, is typically a mixture of descending older stratospheric air and young stratospheric air recently transported isentropically from the tropics. Carbon dioxide is a critically important tracer here not only because its secular trend provides an accurate indicator of the stratospheric age of the older air, but also because its seasonal cycle can uniquely characterize the young stratospheric component [e.g., *Strahan et al.*, 1998; *Andrews et al.*, 2001]. Accordingly, tracer correlations of CO_2 and O_3 should exhibit a latitudinal sensitivity mostly caused by the age and fraction of the younger air in the region. We therefore use tracer correlations with O_3 as a function of latitude to provide stratospheric source profiles for this region.

[20] While we have data from the STRAT and POLARIS campaigns, those data are limited in latitude and longitude coverage. Accordingly, to derive the stratospheric source profiles that exhibit the proper latitudinal dependence we take advantage of the ozonesonde network. Stratospheric source profiles are derived from average ozonesonde profiles from HILO, HI, Wallops Island, VA, Boulder, CO, Goose Bay, Newfoundland, and Churchill, Manitoba. The values of the other tracers as a function of latitude are then derived from aircraft-borne in situ profiles taken during the STRAT and POLARIS campaigns and parameterized as a function of ozone. Additionally, the CO_2 data are adjusted on the basis of the CO_2 secular trend, as measured at tropical ground stations (NOAA Carbon Cycle Greenhouse Gases Group).

3.3. Convective Sources

[21] Air in the lowermost stratosphere transported from midlatitudes and sampled during CRYSTAL-FACE was often impacted by convection, as noted by *Jost et al.*

Table 2. Summary of Convective End-Members Used in Mixing Model Runs b–e

Tracer	Run b	Run c	Run d	Run e
CO_2, ppmv	374.5	374.5	365	374.5
O_3, ppbv	30	30	30	30
CO, ppbv	200	300	125	500
NOy, pptv	3000	8000	8000	5000
H_2O, ppmv	50	200	40	50

[2004]. Evidence for this was often provided by high lightning-induced NO and NOy, as well as high CO and water vapor. Because of the potential for extremely high convective source terms, including ice particles, small fractions of convected air can significantly perturb tracer mixing ratios. *Pfister et al.* [2001] have developed an approach that uses back trajectory calculations combined with GOES infrared imagery to identify when and where the air sampled during CRYSTAL-FACE was influenced by convection. This approach facilitates identifying the time and location of convective systems that could influence the tracer populations of the lowermost stratospheric air sampled over south Florida and would provide the methodology for studying the impact of a recent single convective event on an air mass. However, because we are faced with sampling air that could have been perturbed by more than one convective system, there is no single data set that can provide simultaneously measured tracers for use as convective source terms. We therefore look for an additional way to constrain the convective source terms.

[22] An approach is provided by *Gerbig et al.* [2003], who use a Receptor-Oriented Atmospheric Modeling (ROAM) framework to demonstrate that upper troposphere CO and CO_2 mixing ratios are derived from boundary layer observations that are mixed with tropospheric air during convective ascent into the upper troposphere. ROAM incorporates a backward time Lagrangian particle transport model called the Stochastic Time-Inverted Lagrangian Transport (STILT) Model [*Lin et al.*, 2003] driven with analyzed meteorological fields and parameterized turbulence. Accordingly, we use this approach to help constrain CO and CO_2 values for analysis of the flight of 20020629 (yyyymmdd) The approach of *Pfister et al.* [2001] is used to identify the time, latitude, and longitude of the convective event. Ozone boundary layer values used to constrain convective source values to about 30 ppbv and are based on ground O_3 monitoring stations in geographic regions where convection intersected the back trajectories. However, exceptions to these constraints can for example result from the impact of smoke plumes on CO [*Jost et al.*, 2004].

[23] Constraining the water and NOy convective inputs is much more difficult. The water convective source term is constrained by the smr of the air mass bordering the convective anvil. From *Dessler and Sherwood* [2004, Figure 3] the source term could be limited by an smr of about 200–250 ppmv derived from zonally averaged July 1992 temperatures at 380 K around 55–60°N. However, an increase of just a few degrees from this average along with potential supersaturations could easily increase this maximum to 500 ppmv. We accordingly investigate the model sensitivity to an order of magnitude variation in the convective water source. While the minimum ice saturation ratios experienced on back trajectories would suggest that the water vapor convective input could be further constrained, dilution of the convected air mass with stratospheric air near the convection and along the back trajectory eliminates that constraint. Turning to the NOy convective source term, not only is there a large uncertainty in the contribution to NOy from lightning strokes, there is also a question of the collocation of lightning-induced NO and NOy with the water in the convective cloud. However, plots of cirrus cloud ice water content versus NO and NOy using CRYSTAL-FACE data show reasonable correlations, although with significant cloud-to-cloud variability. Nevertheless, as with water vapor, there is no a priori constraint on the NOy convective source term. We therefore follow a similar approach as with water vapor, testing the model sensitivity to variability in the NOy convective source term of almost an order of magnitude.

[24] Unfortunately, it is difficult if not impossible to attribute observed convective perturbations to a single convective storm. When we extrapolate to an analysis of multiple flights, it is not realistic to identify or characterize the convective events that impact the air masses averaged for the analysis. It therefore becomes even more critical to carry out sensitivity tests for these model runs, by varying the range of convective end-members even beyond values that seem reasonable. We list in Table 2 the range of convective end-members that test the model's sensitivity to their values using tracer data from the 20020629 flight.

3.4. Model Details

[25] Each of the pathways delineated in Figure 1 provide the means for transporting air with a trace gas composition characteristic of a corresponding source region to the lowermost stratosphere over Florida, where it is sampled. The contribution of each of those pathways is proportional to the fraction of air in the sampled air mass from the corresponding source region, which is determined using the mixing model that we describe in the next section. The correspondence between source region, transport pathway, and designation of the source gas composition is given in Table 1.

[26] These source regions do not necessarily represent easily identifiable or meteorologically defined reservoir locations. Distinguishing between air coming from the TTL and lower tropical stratosphere is challenging given the set of measured tracers currently available. We extend the TTL profiles across the tropical tropopause up to 410 K, thus including air that crossed into the lower tropical stratosphere within the past month. We designate as "young stratospheric" air that has entered the stratosphere during the previous six months, and contains H_2O and CO_2 mixing ratios with a strong memory of their respective seasonal cycles. Air with this character was typically observed during the summer over southern California during STRAT. Air designated as "old stratospheric" is predominantly air without the young component, and therefore the correlations used to represent this air are taken from profiles measured in the overworld at midlatitudes. While path 3 is isentropic, and represents equatorward transport of older stratospheric air that has diabatically descended at northern latitudes, the stratospheric source profiles are not derived

from northern latitude data below 380 K in order to avoid contamination from tropospheric air. Instead, they are taken from midlatitude in situ overworld data. Because the slope of tracer isopleths plotted as a function of latitude and potential temperature is about −1 to −1.5 K per degree latitude [see, e.g., *Strahan et al.*, 1998, Figure 5], the midlatitude source profiles must, consistent with diabatic descent, be shifted downward to the isentropes and latitude from which equatorward isentropic transport via path 3 occurs to the lowermost stratosphere over Florida. We use the parameter δK to represent the value, in units of K, of that downward shift in potential temperature (θ). Model runs are carried out to evaluate sensitivity to δK.

[27] To develop the mixing model, we assume that an air mass sampled between 350 and 400 K during CRYSTAL-FACE is a mixture of air masses from the four different source regions: the TTL, the lower tropical and subtropical stratosphere as a source of young stratospheric air, the lower midlatitude and northern midlatitude stratosphere as a source of older stratospheric air, and the troposphere, with the latter region's contribution being convective. Accordingly, we can express any measured tracer mixing ratio as a sum of contributions from the four regions as

$$tr_{TTL} \bullet fr_{TTL} + tr_{ys} \bullet fr_{ys} + tr_{os} \bullet fr_{os} + tr_{conv} \bullet fr_{conv} = tr_{meas} \quad (1)$$

where *tr* represents a measured tracer, *fr* the fraction of air from the source region specified by the subscript, and tr_{meas} is the measured value of the tracer. The model uses a constrained least squares fitting algorithm to minimize the equation $\mathbf{tr} \bullet \mathbf{fr} - \mathbf{tr_m}$, where **tr** is a matrix whose columns are the tracer mixing ratios in air from the different source regions corresponding to the potential temperature for each measurement; **fr** is a vector containing the fractions of air from each component; and $\mathbf{tr_m}$ is a vector containing the mixing ratio of the measured tracers. In this way, the equation is solved independently for each time at which all the tracers are measured. Each tracer is weighted in the fitting algorithm according to its uncertainty relative to its observed range of values in the applicable potential temperature region. The source regions used in the analysis correspond to the 4 illustrated in Figure 1, where the specific latitudes of the air corresponding to ''young'' and ''old'' stratospheric air used in the model runs presented in the manuscript are 20°N and 40–55°N respectively. As previously stated, because we are assuming that the stratospheric components have descended into the lowermost stratosphere from the lower stratosphere, we can vary δK, the descent in potential temperature units for each latitude, but use the same δK for all data points in each flight or model run. We posit that this descent parameter can be 30 K even for young stratospheric air because that air can be rapidly transported poleward to northern latitudes with minimum mixing with older stratospheric air. There, diabatic descend is followed by rapid equatorward isentropic transport.

4. Results and Discussion of Test Model Runs

[28] We choose as a test case the 20020629 ferry flight from Houston to Key West because it provides significant tracer variability within narrow potential temperature bands in the lowermost stratosphere during the flight. Using the various combinations of convective end-member values listed in Table 2, we first present results of model runs that test and illustrate its sensitivity to convective influence and specific convective end-member values. The first model run is free of convective influence, and the next four illustrate the sensitivity to the various convective end-members. Only for run c does the 200 ppmv water vapor convective end-member require mixing with stratospheric air to satisfy constraints imposed by temperatures along back trajectories to avoid saturation conditions that would lead to condensation. Note that measurements within clouds are excluded from the analysis.

[29] We plot in Figure 5a the profile for this flight. The airplane remains at about 14 km (∼354 K) for the first 35 min after climb-out from Houston, ascends to about 15.3 km (∼380 K) for the remainder of the flight, before descending into Key West. The local tropopause during this flight is located between 14.1 and 14.7 km and the aircraft is typically slightly below the tropopause during the first 35 minute leg, and well above the local tropopause for the remainder of the flight until descent into Key West.

[30] In Figures 5b–5f we illustrate the fits to the five tracers for all the data points in the lowermost and lower stratosphere resulting from the five model runs, four of which include convective input using the end-members listed in Table 2. To facilitate the clarity of our discussion, we divide the flight into segments, as shown in Figure 5a. Segment 1, S1, corresponds to the initial cruise portion of the flight near 350 K. The first part of the 380 K cruise portion marks the second segment, S2, of the flight. The third segment of the flight, S3, which begins at about 60,800 s encompasses data where water vapor jumps up to about 10 ppmv and CO to 50 ppbv. The short data gap in the middle is the result of a CO_2 instrument calibration cycle. The fourth segment, S4, begins when the aircraft turns south toward Key West at about 63,000 s. The analysis of *Pfister et al.* [2001] identifies convective influence on back trajectories passing through central west Texas 2–3 days before the data were taken during S1, southwest Texas 1 day before the data were taken during S2, over Arizona 4–5 days prior to the air sampled during the last few minutes of S3, over South Dakota 3–4 days before the data were taken during the first half of S4 and over Idaho 7–8 days the before the data were taken during the latter part of S4. It is interesting that no convective influence was identified during S2 where the water vapor mixing ratio jumped from about 6 to 12 ppmv because this might have served as an excellent opportunity to test the impact of an individual convective event.

[31] Starting with Figure 5b, measured ozone, which is fit well in all the model runs for the entire flight, varies from about 200 to 550 ppbv when the aircraft is near 380 K. The question is what causes the observed variability. Is it the age of stratospheric air that makes up the bulk of these air parcels? Is it the fraction of tropospheric air in the air parcels? Does convective influence play a role? Looking next at CO_2 plotted in Figure 5d, when the aircraft is sampling near 380 K all five model runs fit measured CO_2 reasonably well, although modeled CO_2 is high for runs c and e during S2 and S3 when measured CO_2 is lower, consistent with higher ozone values in older stratospheric

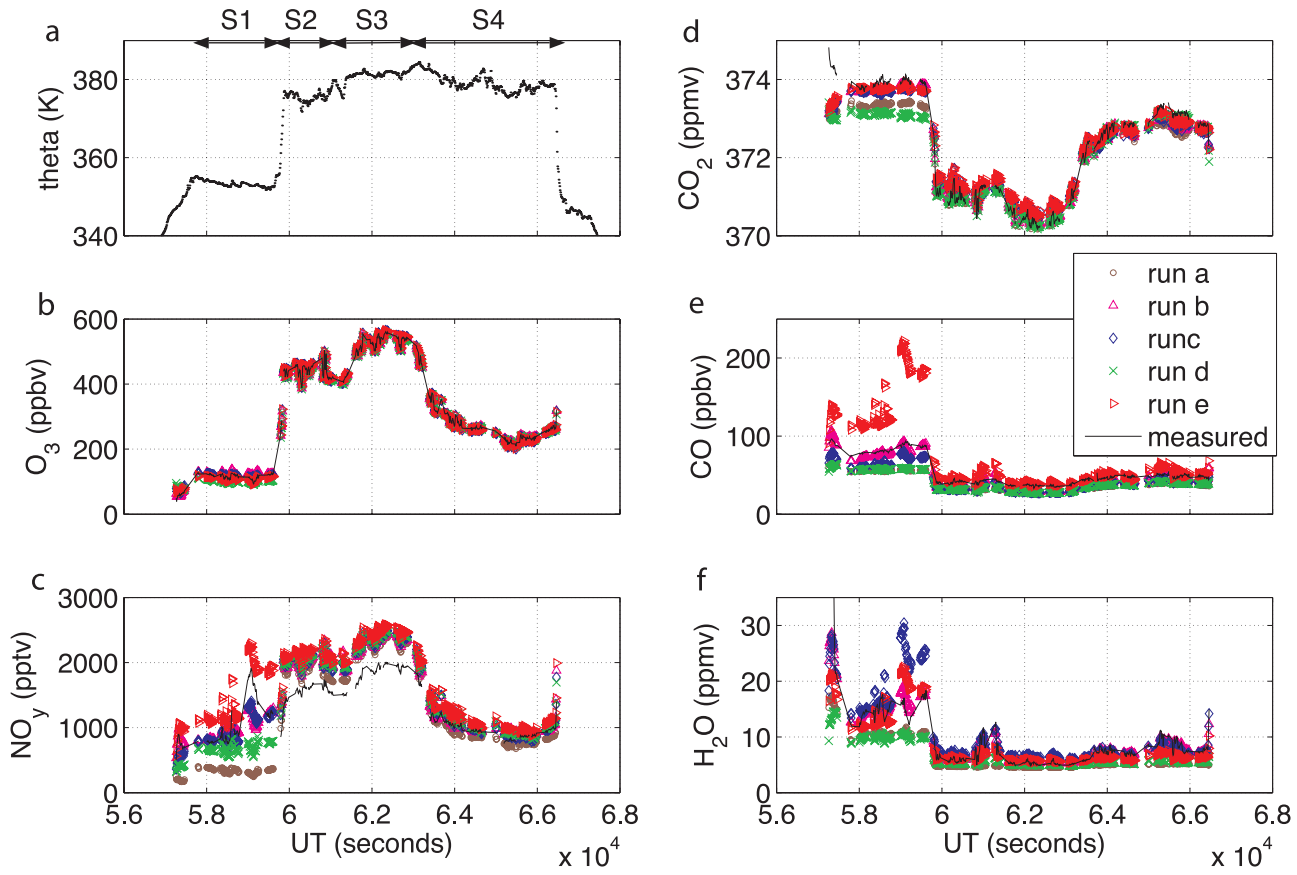

Figure 5. (a) Flight profile, with the different segments of the flight designated as S1–S4. (b–f) Comparisons of the calculated tracer mixing ratios for the five model runs with the measured mixing ratios all plotted versus time during the flight. Model differences for runs b–e that include convection are described in Table 2. The legend, delineating for each tracer the model output for each of the four runs, is valid for all the tracers.

air. During S1 near 350 K, the best fits occur when convection is included in the model with the convective end-member of 374.5 ppmv. Because there is very little old stratospheric air included in the fit during S1, it does not matter which source region for older stratospheric air is used. In contrast however, looking at S2 and S3 for the NOy plots, the best fit occurs in run 2a, with no convective input. This illustrates a level of uncertainty in the source and character of the older stratospheric air. During S1, the NOy fit is good in runs b and c, which include convection, although the very large peak in NOy (with a similar large excursion in NO denoting recent convection) is not matched very well by either run. During S4, all the runs fit very well, because there is virtually no contribution from older stratospheric air. For CO the best fits during S1 are observed during runs b and c when intermediate CO end-members of 200 and 300 ppbv are used. Without convective input during this part of the flight, modeled CO is about 60 to 75% of its measured value. Good agreement for water vapor and CO only result when a convective contribution is included. During S2, S3 and much of S4, CO is too low for all model runs except 2e that uses a CO end-member value of 500 ppbv, suggesting that there is too much older stratospheric air with low CO.

[32] For H_2O, a convective contribution is needed for all segments. It is worth some additional focus on the flight segments near 380 K. During S2, where water vapor jumps up to about 10 ppmv, and CO to 50 ppbv, a convective contribution is necessary to account for these high values while remaining consistent with the high ozone mixing ratios indicative of old stratospheric air. The elevation of water vapor during S4 similarly requires a convective contribution. However, the model suggests that even during S3 when there is 6 to 7 ppmv water, there is a small contribution from convective air. We will investigate later in the manuscript how well we can distinguish between convective influence and wet air isentropically transported from the TTL.

[33] The results plotted in Figure 5 show that including convection in the model is necessary to match the structure of all the tracers throughout the lowermost stratosphere, and model run b provides the best overall fit to the data for the entire flight. However, in some cases different convective source terms provide the best fit during different flight segments. For example, while run b provides the best to measured CO during S1, run e is best during S2 and S3. During S4, run c provides the best fit when the stratospheric contribution to NOy is smaller than in S3, and for CO_2 runs d and e provide the best fit.

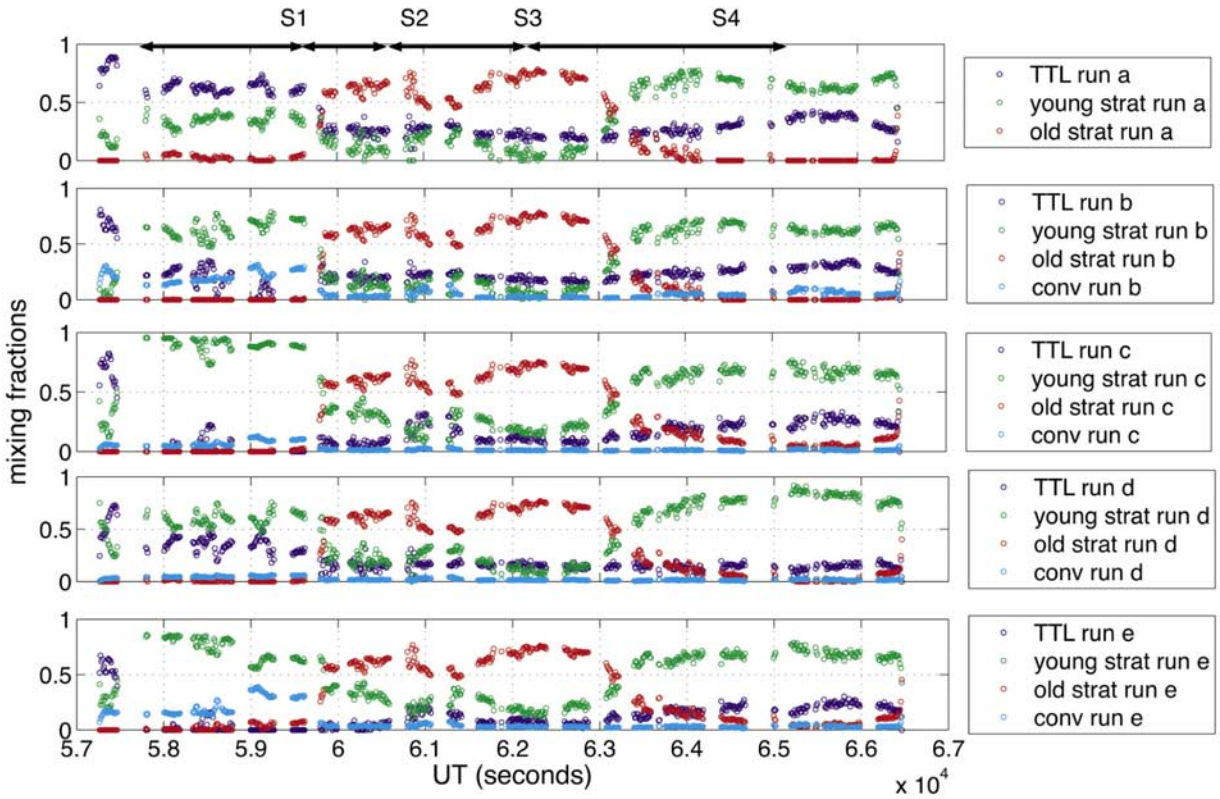

Figure 6. Plots of the fraction of air from each of the four source regions for the different model runs as described in the text with the convective end-members as listed in Table 2. The points are color-coded according to source region, with blue points corresponding to the TTL, green points corresponding to young stratospheric air, red points corresponding to old stratospheric air, and cyan points corresponding to convective air. Model run a uses no convective input. The convective inputs for model runs b–e are as listed in Table 2.

[34] We next address for each run what is the fraction of air from each source region and how much influence does convection have on the source region contributions for each tracer in the model. We plot in Figure 6 the fractions of air from each source region for these model runs. During S1, comparison of run a with the other runs clearly shows that including convection completely alters the composition of the modeled air mass. Without convection the fits to measured H_2O, CO, and NOy are poor and most of the air is from the TTL. When convection is added, TTL air is partially replaced by young stratospheric air that has descended into the lowermost stratosphere. The convective contribution yielded in run d is forced low because of the very low CO_2 source term. During S2, except where convective input has previously been shown to be important, little dependence on convective input is exhibited for the data near 380 K. This forces the TTL contribution to be high. In run c the high water vapor convective source term limits the convective contribution and the TTL contribution as well, pushing up the fraction of young stratospheric air. In run e the high CO convective source term limits the TTL contribution.

[35] Even with the wide range in fit quality during S1 for the four model runs that include convection, it is useful to look at the variability in the convective contribution from each source region to the respective tracer mixing ratios. In Figure 7 we plot the convective fraction of H_2O, CO, and NOy in the sample air mass for each of the model runs. We do not discuss the contributions from convection to O_3 or CO_2, because the impact they have in their respective budgets in the lowermost stratosphere is negligible.

[36] Starting with H_2O, we note that during S1, and neglecting run d that significantly underestimates water vapor, the contribution from convection is about 45% at 58,000 s, near 355 K and about 70% at 59,500 s near 350 K. The data gap just before 59,000 s results from the presence of a cloud, and the high NOy (and NO, not shown) observed until about 59,600 is consistent with a significant contribution from local convection. Run b provides the best fit throughout S1. During the first half of S1, run c also provides a good fit, and taken together these runs suggest that the contribution to water vapor from convection is known to about 20%. When there is high water vapor near 380 K, runs b and c provide good fits and the convective contribution is about 40–50%. During the times when water vapor is 5–6 ppmv near 380 K, runs d and e provide the best fit to water vapor, and the convective contribution is from 10 to 30%. The uncertainty here is about 1 ppmv, in part because the contribution attributed to convection is being driven by other tracers, especially when water is about 5 ppmv where run d provides the best fit. Turning next to CO, during S1 run b provides the best fit and illustrates a 50% convective contribution. For the rest of the flight, run e provides the best fit, although modeled CO is

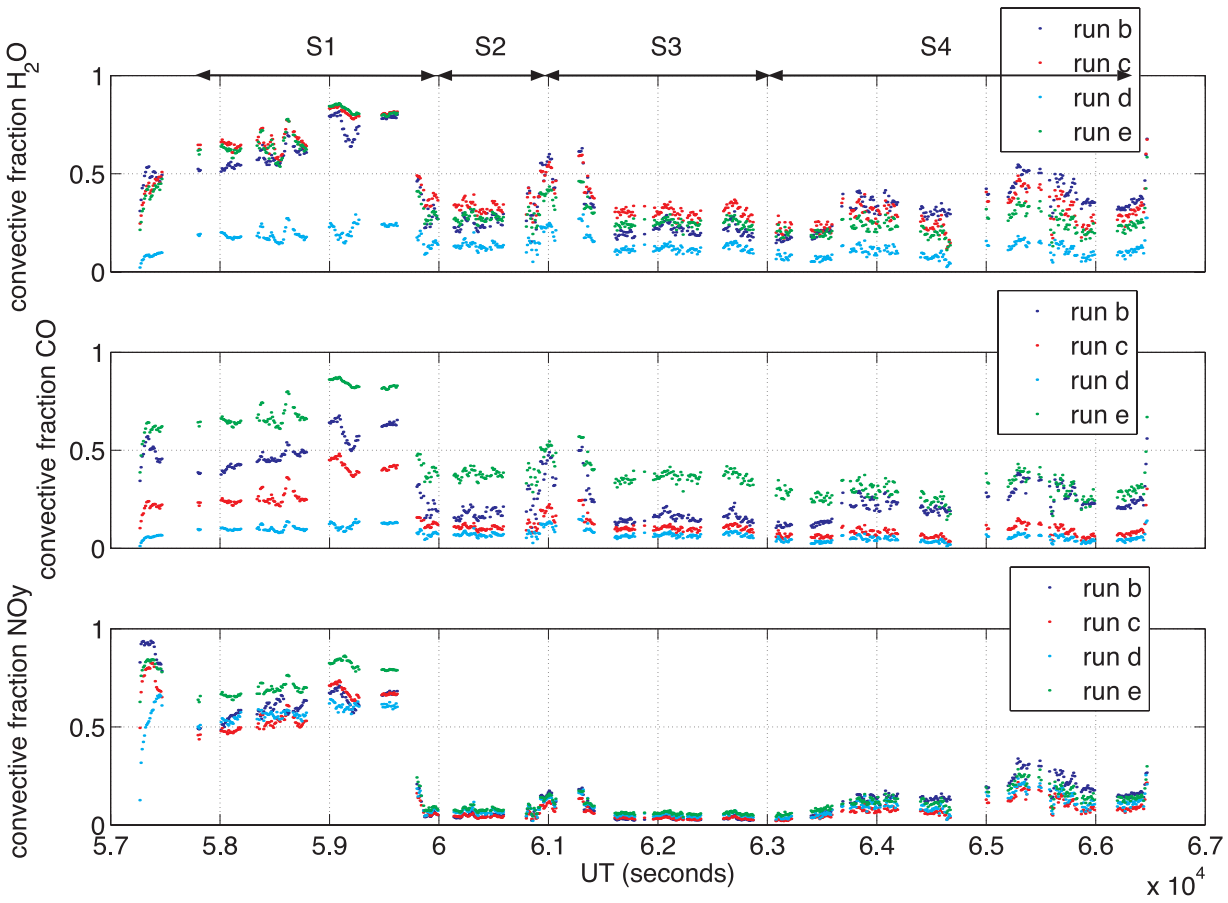

Figure 7. Convective contribution to the listed tracers is plotted versus time for each of the model runs using the convective source terms listed in Table 2.

typically somewhat high, whereas with runs b and c it is somewhat low. Altogether they constrain the convective contribution to be 10–30% near 380 K. For NOy, there is much less disparity in the calculated convective contribution. Even during S1, where the fits to measured NOy range from extremes of about 50% low to 30% high, the convective contribution has a range of about 45 to 90%. When the fit is good, the uncertainty in the convective contribution is much less. For the sampling region near 380 K, the convective contribution is about 5–30% and for the most part this variability is real and dependent more on the air mass than the model fit. The ultimate question that we will address later in the manuscript is how this convective contribution varied throughout the mission.

5. Results and Discussion of Mission Analysis

[37] Instead of combining all the CRYSTAL-FACE data for this analysis, we categorize the results according to the study by *Pittman et al.* [2004, 2007] that uses back trajectory calculations and tracer-tracer correlations to illustrate the changes that took place during July in the pathways transporting air into the lowermost stratosphere over Florida. On the basis of the analysis from *Pittman et al.* [2004], and as shown in Figure 3, the flight data can be separated into three regimes during the beginning, middle, and end of the month, for which back trajectories indicate the predominance of distinctly different transport pathways. For the first part of July, corresponding to the flights on 29 June and 3, 7, and 9 July, trajectories brought air to South Florida from eastern Canada, and from the western United states passing through latitudes up to 50°N. For the middle part of July, corresponding to flights on 11, 16, 19, and 21 July, most of the air came from of the California coast, passing through latitudes from 50 to 65°N. Some of that air detoured over Texas before heading to South Florida. During the latter part of the month, corresponding to flights on 23, 26, 28, and 29 July, the source of air is more variable, with the major sources of air being the subtropical Pacific and Atlantic, and a minor source being eastern Canada. To investigate the impact of these three trajectory patterns, we bin the tracer data in 1° units of potential temperature for each of the three regimes. We then determine for each regime the best fit as for the example on 20020629. We show in Table 3 the convective source terms that provide the best overall fit for the data in each of the three regimes.

[38] Using these source terms and assuming δK values of 30 K for both the younger (from 20°N) and older (from 45°N) stratospheric air source terms, we show in Figure 8 the model results for the three regimes. In each panel we plot the average value of the tracer binned in 1 K units, the comparable tracer mixing ratios from the model, and, except for CO_2, the contribution from each source region. We only show the agreement between measured and modeled CO_2.

Table 3. Convective End-Members for the Model Runs for Data During Each Regime

Tracer	Convective Source Terms for Regime 1	Convective Source Terms for Regime 2	Convective Source Terms for Regime 3
CO_2, ppmv	374.5	374.5	374.5
O_3, ppbv	30	30	30
CO, ppbv	500	350	300
NOy, pptv	3000	12000	6000
H_2O, ppmv	200	125	200

Because the fractional difference in CO_2 corresponding to the different source regions is so small, the fractional contributions to CO_2 from each of these regions is virtually the same as the fraction of air from each source region plotted in Figure 9. In Figure 8 (bottom right), we plot the fraction of convective air for the three tracers for which convection can be the dominant source.

[39] Looking at water vapor first, the most surprising result from the model is that even around 380 to 390 K, the convective contribution is significant. The water vapor mixing ratio increases sharply with decreasing potential temperature, starting at about 388 K. This increase might normally be thought to be a result of air from the tropics not being dehydrated to the expected 6 to 7 ppmv. In fact, if this were the case, the air would have to be purely tropical in character, and ozone would be much less than the observed 350 to 450 ppbv. The model reveals that both convected and older stratospheric air are required to provide a satisfactory fit. While the model does show that young stratospheric air dominates above 390 K, TTL air is present up to 410 K as well. However, results in this region are more uncertain than those below 390 K. There is a very significant convective contribution to NOy and CO as well, increasing with decreasing potential temperature, similar to water vapor. The CO contribution and its implications have already been thoroughly discussed by *Jost et al.* [2004]. The NOy contribution is of interest because NO from lightning is the source of this NOy and during its approximately weeklong lifetime in the summertime UT/LS, it can impact ozone loss by either converting active chlorine to chlorine nitrate, thereby reducing ozone loss, or by removing ozone through the NOx catalytic cycle. However, most of the NOy in the lowermost stratosphere is attributable to old stratospheric air.

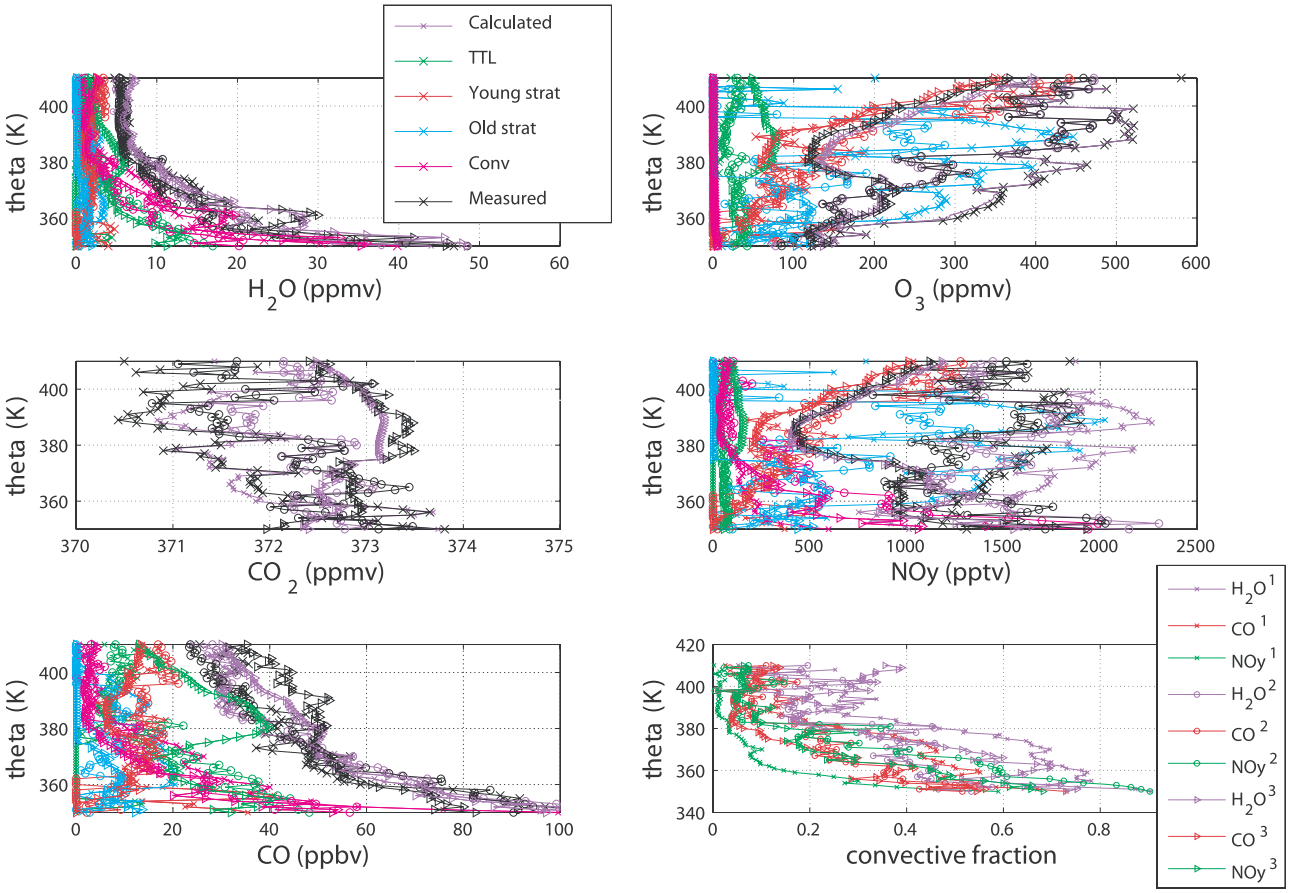

Figure 8. Plots during the three regimes of the average value of the tracer binned in 1 K units, the comparable calculated tracer mixing ratios, and, except for CO_2, the contribution from each source region. For CO_2, only the agreement between measured and modeled CO_2 is shown. The color coding in the legend in the top left plot is valid for each of the tracer versus theta plots. The bottom right plot shows the fraction of H_2O, CO, and NOy from convection using the convective values for each regime (1–3) shown in Table 3. The symbols used to represent data from the three regimes in the bottom right plot are similarly used in all the plots.

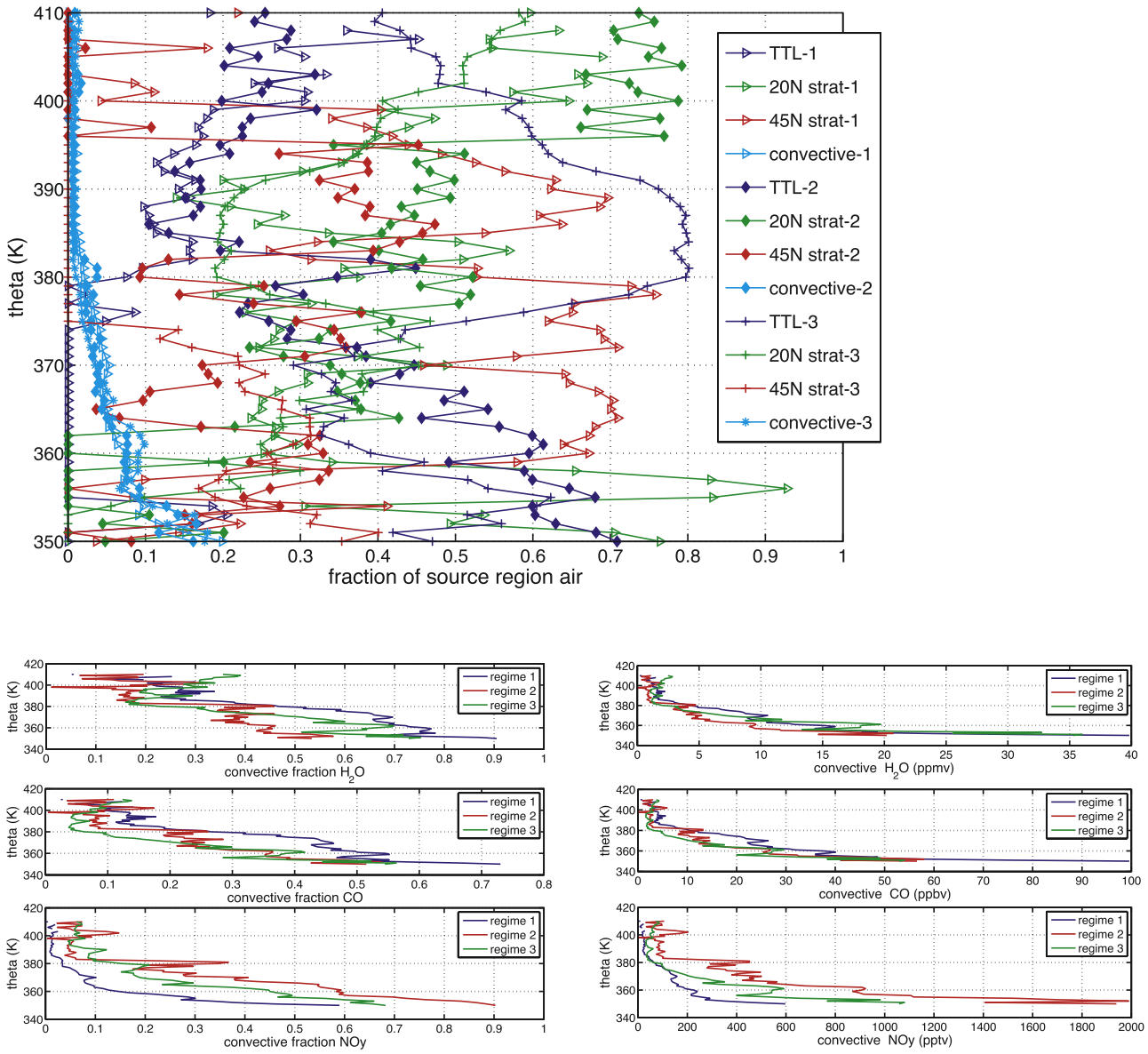

Figure 9. (top) Fraction of air from each source region is plotted for each regime. The legend identifies contribution from each of the source regions for the three regimes separated by time during the month of July. (bottom left and right) Convective contribution to the listed tracers is plotted for each regime in fractional and absolute terms.

[40] Because there is intense interest in the control of midlatitude ozone in the lowermost stratosphere we need to carefully explore the implications of the model on ozone. It is clear that a small fraction of convected air does not significantly influence ozone in the lowermost stratosphere, because typically the ozone content of convected air is only somewhat less than that of TTL air. The model shows that in regime 1 older stratospheric air not unexpectedly provides most of the ozone, with young stratospheric air the source of the remainder. There is one feature just above 380 K with an increase in young air, as identified by decreasing ozone and NOy, and increasing CO_2. What is clear is that ozone variability can be very large in the lowermost stratosphere and ozone values are controlled by the amount of older stratospheric air. Accordingly and not unexpectedly, the strength of the summer monsoon will strongly impact measured ozone in the midlatitude lowermost stratosphere.

[41] In comparing the model results during regime 2, with regime 1, we note that during regime 2 there is a lower fraction of older stratospheric air than in regime 1, and the convective contribution above 370 K has decreased as well. Below 370 K, (midlatitude) convection dominates as the NOy source because there is both more NOy from convection and less old stratospheric air than in regime 1. For CO and water vapor, the TTL and convective sources contribute about the same as in regime 1. These results suggest that even though the back trajectories above 370 K in regime 2 more consistently traverse higher latitudes than in regime 1, it is the intersection of convection along the back trajectories during regime 1 that provides the turbulent mixing

responsible for the mixing of both older stratospheric and convective air into the sampled air parcels.

[42] Looking at the model results for regime 3, the contribution of older stratospheric air has decreased even further near 380 K, but between 360 and 370 K the feature still remains about the same as in regime 2. The model shows that near 380 K, TTL air is the dominant source of CO and water vapor. CO and water vapor decrease as TTL air is replaced by older stratospheric air below 370 K, and then increase as both the TTL and convective contributions increase with decreasing potential temperature.

[43] Next we show in Figure 9 the fraction of air from each source region during each regime for averaged air masses within each θ bin. This plot most clearly illustrates the largest contribution of old stratospheric air during regime 1 as well as the transition to a large TTL component between 380 and 390 K in regime 3. It is interesting to note that during regime 1 there is virtually no attribution to TTL air and except for a unique contribution during regime 1 between 350 and 360 K, the contribution of young stratospheric air declines with θ as one might expect. The model increases the contribution of young stratospheric air in this region, rather than TTL air, because of relatively high CO coupled with an increase in CO_2. The seasonal cycle of CO_2 helps constrain the model to use young stratospheric air rather than TTL air.

[44] Additionally, we note that the model identifies 50 to 60% of the air around 355 K as young stratospheric air. Because this result is unexpected, we investigate how robust this feature is to both the age of the young stratospheric air and the chosen convective source terms. All the stratospheric tracer profiles were derived from summertime STRAT and POLARIS data. This does not allow for the possibility, or indeed the probability, that the average time it takes air between 380 and 420 K and between 30 and 45°N to travel poleward to about 60°N while radiatively descending about 30–40 K could be a few months [*Spackman et al.*, 2007]. This transit time can be assessed by carefully comparing CO_2 and water vapor mixing ratios in the two regions of interest, because their respective seasonal cycles can help resolve the different transit times [*Boering et al.*, 1995]. Analysis of the limited lowermost stratospheric data available from POLARIS shows that the young component of the air entered the tropical stratosphere in the spring. This represents a transit time from the tropical tropopause region consistent with that shown by the lowermost stratospheric air sampled during POLARIS at high latitudes. While this validates the reference profiles used for midlatitude stratospheric air, we tested the model sensitivity to the seasonal dependence of CO_2 and H_2O profiles. The substitution of O_3:CO_2 and O_3:H_2O correlations derived from spring midlatitude stratosphere POLARIS data resulted in negligible differences to the model fits.

[45] The convective contribution during all three regimes appears to be virtually identical, contributing about 0.7% of the air just above 380 K, and gradually increasing with decreasing θ to about 8% near 360 K, and 18% at 350 K. However, it is not only the fraction of air but also the actual tracer contribution that is important. In Figure 9 (bottom left) we illustrate how the convective contribution to water vapor, carbon monoxide, and NOy differ during the three regimes. For example, between 360 and 380 K, regime 1 is mostly older stratospheric air. The convective contribution to water vapor is highest during this regime from a fractional perspective, averaging about 65%, somewhat lower during regime 2, averaging about 40%, and extremely altitude-dependent in regime 3. However, from an absolute standpoint, it is somewhat lower during regime 2 than regimes 1 and 3. This contrasts with NOy, for which the highest contribution is during regime 2. The convective contribution to CO, like water vapor, is highest in regime 1. These results are consistent with the possibility that during regime 2 more extensive lightning accompanying deep convection to higher altitudes is the source of higher NOy than is observed during regime 1.

[46] While Figures 8 and 9 show that there are differences in the convective contributions in the three regimes, do these differences correlate with the fraction of old stratospheric air, thus suggesting that mixing caused by convection increases the mixing in of stratospheric air? For example, the air mass in regime 1 between 360 and 380 K is mostly old stratospheric air, and water vapor and CO show a commensurate increase in convective influence, whereas NOy does not. The convective contribution of water vapor and CO also show a dip below 360 K, in agreement with the transition to the decrease in older stratospheric air. In regime 2, the increase in old stratospheric air occurs sharply at 390 K, yet the increase in convective influence occurs sharply at 380 K, thus imposing an upper bound on the convection that contributed to the sampled air masses. A comparison of the fraction of old stratospheric air in regimes 2 and 3 show a crossing around 370 K with the air sampled during regime 3 more influenced by older stratospheric air below 370 K and regime 2 above 370 K. The relative fraction of convective influence at least for water vapor and CO are broadly consistent with this. Additionally, convection in southern Canada in the vicinity of intense forest fires were responsible for the highest CO detected during CRYSTAL-FACE near 380 K [*Jost et al.*, 2004]. It is convection at these northern latitudes that has the potential for depositing the most water vapor in the lowest stratosphere as well.

[47] Model runs (not shown) illustrate that variations in convective end-members that still provide good fits to the tracer data do not significantly affect the conclusions regarding the importance of convection in the budgets of H_2O, CO, and NOy for the data in the lowermost stratosphere. Similarly, the age of the stratospheric air that has descended into the lowermost stratosphere had only a modest impact on the results and does not significantly impact modeled convective influence. The combination of the sensitivity tests indicates that even without being able to constrain the convective source term values, the convective contribution of each tracer to the lowermost stratosphere is constrained by the model.

6. Summary and Conclusions

[48] As illustrated in Figure 1, air can be transported into the lowermost stratosphere from different source regions via different dynamical mechanisms. These mechanisms are known to exhibit both seasonal and longitudinal dependences and their response to a changing global climate needs to be understood for prediction of a potential impact on

ozone depletion, cirrus cloud climatology, and the radiative properties of the region. Developing a framework for quantifying the effect of each of these mechanisms represents the first step in evaluating and improving their parameterizations in trajectory models. We have shown how a box model with a constrained least squares fitting algorithm that fits long-lived tracer mixing ratios measured simultaneously in the lowermost and lower stratosphere can successfully characterize the chemical composition of the sampled air mass according to source region.

[49] Using this model we show that (1) during much of CRYSTAL-FACE, older stratospheric air transported equatorward around the North American monsoon is the major component of air in the lowermost stratosphere over Florida; (2) tracer-tracer correlations can help constrain the convective end-members used as input source terms for model analysis of an air mass perturbed by an individual convective or cumulative events; (3) air convected up to and above 380 K at northern midlatitudes that is transported by the monsoon circulation provides a significant flux of H_2O, NOy, and CO throughout the subtropical and midlatitude lowermost stratosphere and into the overworld; and (4) while the fraction of convective air in the sampled air masses is small, and not tightly constrained by the model, the fractions of convectively transported H_2O, CO, and NOy are tightly constrained and surprisingly insensitive to the choice of convective source terms. The combination of convective injection and equatorward transport provides a potential for these and other boundary layer species to enter the tropics and ascend into the stratosphere as part of the Brewer-Dobson circulation, with water vapor bypassing the tropical tropopause cold trap.

[50] These results, which address the cumulative effect of convection, complement those of *Ray et al.* [2004] in which analysis of the impact of smoke plumes convected into the lower midlatitude stratosphere was carried out using tracer measurements and tracer-tracer correlations. On the basis of a determination of the tropospheric content of a convected plume to be 25%, and assumptions on its size, Ray et al. are able to calculate the mass flux into the stratosphere from an individual convective event.

[51] It is clear from this study that the variability in the age and fraction of the stratospheric component is likely a prime reason for ozone variability in the lowermost stratosphere both longitudinally and seasonally. While small contributions of tropospheric air can reduce ozone, small contributions of older stratospheric air can similarly increase it. The results shown here specifically illustrate how the North American summer monsoon has both a significant impact on ozone in the northern midlatitude lower stratosphere via equatorward transport of ozone-rich air and on water vapor through convection, followed by mixing with stratospheric air, and subsequent equatorward transport. Moreover, as Figures 8 and 9 show, high concentrations of water vapor reach the lowermost stratosphere through convective injection, and can provide, in combination with low temperatures, the site for rapid, surface-catalyzed conversion of inorganic chlorine to free radical form. Even with current controls on fluorocarbon emissions and projected stratospheric ozone recovery, this must bring into focus the sensitivity of catalytic ozone loss to the coupling of the chlorine/bromine radical systems through the $ClO + BrO \rightarrow Cl + Br + O_2$ rate limiting step with water vapor amplified by convection and the potential impact that climate change will have on these heterogeneous processes that catalytically destroy ozone. Results during CRYSTAL-FACE documenting midlatitude convection extending above 380 K [*Jost et al.*, 2004] suggest that cirrus could be found there as well. Changes in the strength of the North American monsoon, as well as in the extent and strength of northern midlatitude convection resulting from surface warming could result in a dynamically induced change in ozone mixing ratios.

[52] The results described in this manuscript provide important implications for potential impact of global change both on midlatitude ozone through the convectively induced increase in water vapor and NOx in the lowermost stratosphere, through the relative strengths of transport pathways into the region, and through increases in stratospheric water vapor from a combination of midlatitude convection and equatorward flow. As stated by *Gettelman et al.* [2004], chemical transport model results suggest that results similar to these would be amplified in the stronger Asian monsoon. In fact, *Dethof et al.* [1999] have identified a mechanism for moistening the lower stratosphere involving the Asian monsoon whereby monsoon convection moistens the upper troposphere and filaments of moist air are subsequently drawn into the lower stratosphere. Furthermore, *Fu et al.* [2006] use CO and water vapor data from the Microwave Limb Sounder aboard the Aura satellite to show that during boreal summer water vapor and CO are convectively transported into the lower stratosphere over the Tibetan Plateau from where diabatic trajectory studies suggest air rises and travels equatorward where it joins the general circulation. The response of these convective processes and the Asian monsoon to global climate change has been of considerable interest because of its impact on rainfall amounts on the Asian continent [*Intergovernmental Panel on Climate Change*, 2001]. They are of interest here because of their impact on midlatitude ozone and stratospheric water vapor.

[53] Because the monsoon is driven by thermal gradients between hot landmasses and colder oceans, it has been suggested [*Kumar et al.*, 1999] that monsoon circulations will strengthen with increased surface temperatures. Stronger monsoon circulation could result in more of the air convected into the overworld reaching the inner tropics, as is already occurring in MOZART3 model simulations described by *Gettelman et al.* [2004]. Predicting the impact on the midlatitude lowermost stratosphere and the lower subtropical stratosphere to increased monsoon circulation as well as the convection associated with it primarily requires sufficient understanding of their current impact.

[54] One of the most interesting results from the model is that the water vapor contribution from convection is significant even up to 380 K, and the feature is robust. While the comparable NOy contribution is less robust, in part because there are large uncertainties in the convective source terms and significant uncertainties in the stratospheric source terms, the analysis does show that convection is a significant source of NOx up to 380 K as well.

[55] **Acknowledgments.** We appreciate the efforts of the WB-57 crew and pilots as well as all those who helped make the CRYSTAL-FACE mission so successful. Additional thanks to Don Anderson for recognizing

the capacity, utility, and strengths of the WB-57 aircraft and Kathy Thompson for arranging the Harvard team's home away from home. Thanks to Ed Hare and the World Ozone and Ultraviolet data center for ozonesonde data. Support from NASA grants NAG5-11548, NAG5-115487, NAG5-8779, and NAG1-01095 is gratefully acknowledged.

References

Andrews, A. E., K. A. Boering, S. C. Wofsy, B. C. Daube, D. B. Jones, S. Alex, M. Loewenstein, J. R. Podolske, and S. E. Strahan (2001), Empirical age spectra for the midlatitude lower stratosphere from in situ observations of CO_2, *J. Geophys. Res.*, *106*, 10,257–10,274.

Bannister, R., A. O'Neill, A. Gregory, and K. Nissen (2004), The role of the S. E. Asian monsoon and other seasonal features in creating the tape-recorder signal in the Unified Model, paper presented at Third SPARC General Assembly, Stratospheric Processes and Their Role in Clim., World Clim. Res. Programme, Victoria, B.C., Canada, Aug.

Boering, K. A., B. C. Daube, S. C. Wofsy, M. Loewenstein, J. R. Podolske, and E. R. Keim (1994), Tracer-tracer relationships and lower stratospheric dynamics: CO_2 and N_2O correlations during SPADE, *Geophys. Res. Lett.*, *21*, 2567–2570.

Boering, K. A., E. J. Hintsa, S. C. Wofsy, J. G. Anderson, B. C. Daube Jr., A. E. Dessler, M. Loewenstein, M. P. McCormick, J. R. Podolske, E. M. Weinstock, and G. K. Yue (1995), Measurements of stratospheric carbon dioxide and water vapor at northern midlatitudes: Implications for troposphere-to-stratosphere transport, *Geophys. Res. Lett.*, *22*, 2737–2740.

Boering, K. A., et al. (1996), Stratospheric mean ages and transport rates from observations of carbon dioxide and nitrous oxide, *Science*, *274*, 1340–1343.

Bojkov, R. D., and V. E. Fioletov (1997), Changes of the lower stratospheric ozone over Europe and Canada, *J. Geophys. Res.*, *102*, 1337–1347.

Christian, H. J., et al. (2003), Global frequency of lightning as observed from space by the Optical Transient Detector, *J. Geophys. Res.*, *108*(D1), 4005, doi:10.1029/2002JD002347.

Conway, C. L., et al. (2003), Carbon cycle greenhouse gases, *CMDL Summary Rep. 27*, chap. 2, NOAA Clim. Monit. and Diagn. Lab., Boulder, Colo.

Cooper, O., et al. (2004), A case study of trans-pacific warm conveyor belt transport: The influence of merging airstreams on trace gas import to North America, *J. Geophys. Res.*, *109*, D23S09, doi:10.1029/2003JD004006.

Dessler, A. E., and S. C. Sherwood (2004), The effect of convection on the summertime extratropical lower stratosphere, *J. Geophys. Res.*, *109*, D23301, doi:10.1029/2004JD005209.

Dessler, A. E., E. J. Hintsa, E. M. Weinstock, J. G. Anderson, and K. R. Chan (1995), Mechanisms controlling water vapor in the lower stratosphere: "A tale of two stratospheres," *J. Geophys. Res.*, *100*, 23,167–23,172.

Dethof, A., A. O'Neill, J. M. Slingo, and H. G. J. Schmit (1999), A mechanism for moistening the lower stratosphere involving the Asian summer monsoon, *Q. J. R. Meteorol. Soc.*, *125*, 1079–1106.

Dunkerton, T. (1995), Evidence of meridional motion in the summer lower stratosphere adjacent to monsoon regions, *J. Geophys. Res.*, *100*, 16,675–16,688.

Fu, R., Y. Hu, J. S. Wright, J. H. Jiang, R. E. Dickinson, M. Chen, M. Filipiak, W. G. Read, J. W. Waters, and D. L. Wu (2006), Short circuit of water vapor and polluted air to the global stratosphere by convective transport over the Tibetan plateau, *Proc. Natl. Acad. Sci. U. S. A.*, *103*, 5664–5669.

Gerbig, C., J. C. Lin, S. C. Wofsy, B. C. Daube, A. E. Andrews, B. B. Stephens, P. S. Bakwin, and C. A. Grainger (2003), Toward constraining regional-scale fluxes of CO_2 with atmospheric observations over a continent: 2. Analysis of COBRA data using a receptor-oriented framework, *J. Geophys. Res.*, *108*(D24), 4757, doi:10.1029/2003JD003770.

Gettelman, A., D. E. Kinnison, T. J. Dunkerton, and G. P. Brasseur (2004), Impact of monsoon circulations on the upper troposphere and lower stratosphere, *J. Geophys. Res.*, *109*, D22101, doi:10.1029/2004JD004878.

Hanisco, T. F., E. J. Moyer, E. M. Weinstock, J. M. St.Clair, D. S. Sayres, J. B. Smith, R. Lockwood, and J. G. Anderson (2007), Observations of deep convective influence on stratospheric water vapor and its isotopic composition, *Geophys. Res. Lett.*, *34*, L04814, doi:10.1029/2006GL027899.

Hintsa, E. J., E. M. Weinstock, A. E. Dessler, J. G. Anderson, M. Loewenstein, and J. R. Podolske (1994), SPADE H_2O measurements and the seasonal cycle of water vapor, *Geophys. Res. Lett.*, *21*, 2559–2562.

Hintsa, E. J., et al. (1998), Troposphere-to-stratosphere transport in the lowermost stratosphere from measurements of H_2O, CO_2, N_2O and O_3, *Geophys. Res. Lett.*, *25*, 2655–2658.

Holton, J. R., P. H. Haynes, M. E. McIntyre, A. R. Douglass, R. B. Rood, and L. Pfister (1995), Stratosphere-troposphere exchange, *Rev. Geophys.*, *33*, 403–439.

Intergovernmental Panel on Climate Change (2001), *Climate Change 2001: The Scientific Basis*, 892 pp., edited by J. T. Houghton et al., Cambridge Univ. Press, New York.

Jensen, E., and L. Pfister (2004), Transport and freeze-drying in the tropical tropopause layer, *J. Geophys. Res.*, *109*, D02207, doi:10.1029/2003JD004022.

Jost, H.-J., et al. (2004), In-situ observations of mid-latitude forest fire plumes deep in the stratosphere, *Geophys. Res. Lett.*, *31*, L11101, doi:10.1029/2003GL019253.

Kumar, K. K., B. Rajagopalan, and M. A. Cane (1999), On the weakening relationship between the Indian monsoon and ENSO, *Science*, *284*, 2156–2159, doi:10.1126/science.284.5423.2156.

Lane, T. P., R. D. Sharman, T. L. Clark, and H.-M. Hsu (2003), An investigation of turbulence generation mechanisms above deep convection, *J. Atmos. Sci.*, *60*, 1297–1321.

Lin, J. C., C. Gerbig, S. C. Wofsy, A. E. Andrews, B. C. Daube, K. J. Davis, and C. A. Grainger (2003), A near-field tool for simulating the upstream influence of atmospheric observations: The Stochastic Time-Inverted Lagrangian Transport (STILT) model, *J. Geophys. Res.*, *108*(D16), 4493, doi:10.1029/2002JD003161.

Logan, J. A., et al. (1999), Trends in the vertical distribution of ozone: A comparison of two analyses of ozonesonde data, *J. Geophys. Res.*, *104*(D21), 26,373–26,400.

Pfister, L., et al. (2001), Aircraft observations of thin cirrus clouds near the tropical tropopause, *J. Geophys. Res.*, *106*, 9765–9786.

Pittman, J. V., et al. (2004), Identifying transport mechanisms of air into the subtropical lowermost stratosphere during the summertime, paper presented at Third SPARC General Assembly, Stratospheric Processes and Their Role in Clim., World Clim. Res. Programme, Victoria, B. C., Canada, Aug.

Pittman, J. V., et al. (2007), Transport in the subtropical lowermost stratosphere during the Cirrus Regional Study of Tropical Anvils and Cirrus Layers–Florida Area Cirrus Experiment, *J. Geophys. Res.*, *112*, D08304, doi:10.1029/2006JD007851.

Poulida, O., R. R. Dickerson, and A. Heymsfield (1996), Stratosphere-troposphere exchange in a midlatitude mesoscale convecive complex: 1. Observations, *J. Geophys. Res.*, *101*, 6823–6836.

Ray, E. A., F. L. Moore, J. W. Elkins, G. S. Dutton, D. W. Fahey, H. Vömel, S. J. Oltmans, and K. H. Rosenlof (1999), Transport into the Northern Hemisphere lowermost stratosphere revealed by in situ tracer measurements, *J. Geophys. Res.*, *104*(D21), 26,565–26,580.

Ray, E. A., et al. (2004), Evidence of the effect of summertime midlatitude convection on the subtropical lower stratosphere from CRYSTAL-FACE tracer measurements, *J. Geophys. Res.*, *109*, D18304, doi:10.1029/2004JD004655.

Richard, E. C., K. C. Aikin, E. A. Ray, K. H. Rosenlof, T. L. Thompson, A. Weinheimer, D. Montzka, D. Knapp, B. Ridley, and A. Gettelman (2003), Large-scale equatorward transport of ozone in the subtropical lower stratosphere, *J. Geophys. Res.*, *108*(D23), 4714, doi:10.1029/2003JD003884.

Spackman, J. R., E. M. Weinstock, J. G. Anderson, D. F. Hurst, H.-J. Jost, and S. M. Schauffler (2007), Aircraft observations of rapid meridional transport from the tropical tropopause layer into the lowermost stratosphere: Implications for midlatitude ozone, *J. Geophys. Res.*, *112*, D12308, doi:10.1029/2006JD007618.

Strahan, S. E., A. R. Douglas, J. E. Nielsen, and K. A. Boering (1998), The CO_2 seasonal cycle as a tracer of transport, *J. Geophys. Res.*, *103*, 13,729–13,741.

Wang, P. K. (2003), Moisture plumes above thunderstorm anvils and their contributions to cross-tropopause transport of water vapor in midlatitudes, *J. Geophys. Res.*, *108*(D6), 4194, doi:10.1029/2002JD002581.

J. G. Anderson, D. S. Sayres, J. B. Smith, and E. M. Weinstock, Department of Chemistry and Biological Chemistry, Harvard University, Cambridge, MA 02138, USA. (elliot@huarp.harvard.edu)

B. C. Daube and S. C. Wofsy, Department of Earth and Planetary Sciences, Harvard University, Cambridge, MA 02138, USA.

C. Gerbig, Max-Planck Institute for Biogeochemistry, D-07745 Jena, Germany.

H.-J. Jost, NovaWave Technologies, Redwood City, CA 94065, USA.

M. Loewenstein, J. P. Lopez, and L. Pfister, NASA Ames Research Center, Moffett Field, CA 94035, USA.

J. V. Pittman, NASA Marshall Space Flight Center, Huntsville, AL 35812, USA.

E. C. Richard, Laboratory for Atmospheric and Space Physics, University of Colorado, Boulder, CO 80303, USA.

B. A. Ridley and A. J. Weinheimer, Atmospheric Chemistry Division, National Center for Atmospheric Research, Boulder, CO 80307, USA.

T. L. Thompson, Earth System Research Laboratory, NOAA, Boulder, CO 80305, USA.

I. Xueref, Laboratoire des Sciences du Climat et de l'Environment, Commissariat l'Energie Atomique, F-91191 Gif-Sur-Yvette Cedex, France.